Monitoring and quantifying crack-based light damage in masonry walls with digital image correlation

Korswagen, Paul A.; Rots, Jan G.

DOI
10.1007/978-981-15-9121-1_1

Publication date
2021

Document Version
Accepted author manuscript

Published in
Proceedings of 1st International Conference on Structural Damage Modelling and Assessment - SDMA 2020

Monitoring and quantifying crack-based light damage in masonry walls with Digital Image Correlation

Paul A. Korswagen [1,*], Jan G. Rots [1],

[1] *Materials, Mechanics, Management & Design (3MD), Delft University of Technology, The Netherlands*

* *Corresponding author: p.a.korswageneguren@tudelft.nl*

Abstract: Recent, induced earthquakes in the north of the Netherlands have led to a large number of damage claims. Many claims can be considered to fall into the category of 'light damage' to the ubiquitous, unreinforced masonry structures in the region. To evaluate and predict the behaviour of cracks, characteristic of light masonry damage, caused by seismic or other actions, an experimental campaign, linked to the validation of computational models, has been pursued.
To accurately capture the initiation of visible cracks, wider than 0.1mm, Digital Image Correlation (DIC) was applied to monitor the entire surface of full-scale wall panels and smaller specimens. Moreover, an optimised speckle pattern and solving algorithm was developed to be able to monitor not only the initiation, but also the propagation of the cracks during subsequent (repeating) loading cycles.
In this approach, the crack data is then used to characterise the intensity of damage with a single scalar; the parameter, denoted Ψ and comprising the number, width and length of the cracks, is used to evaluate the progression of light damage in experiments and finite element models. A description of the DIC technique applied and of the development and usage of the damage parameter for masonry is presented herein.

Keywords: Masonry, Cracks, Light Damage, DIC

1. Introduction

Structures of all kinds are subjected to actions that have the potential of causing damage whenever these lead to undesired conditions in the structures. In general, any state deviating from the original state or the intended state of a structure can be categorised as damage. The deviating state can be a direct result of a particular action on a structure or its components. Loss of strength due to cracks in walls, crushing of bricks or loss of elements, as well as loss of section due to chemical action or freezing, or high distortions due to creep behaviour or overloading, are all examples of damage in masonry structures.

When observing minor levels of damage, strategies developed for near-collapse or ultimate limit states (like surveying if there is a severe loss of strength or excessive distortion of the structure) may fail to accurately describe minor damage. Additionally, these expressions of damage may not be readily detectable or are difficult to assess by an inexperienced observer or inspector. Cracking, on the other hand, the occurrence of cracks and fissures on or through walls and other elements in a masonry structure, is easily observable and directly relatable to some degree of damage. Moreover, many phenomena such as earthquakes or settlements are commonly observed to cause cracking. Consequently, many studies [e.g. 4, 5, 14, 18, 25, 26] have opted for the consideration of cracks as a measure for the evaluation of (minor) damage; where, put simply: the absence of cracks corresponds to no damage, a few small cracks to very light damage, and larger cracks to more intense damage.

Nonetheless, even if a clear expression of damage such as cracking, is set, the quantitative evaluation of the damage remains unclear. It is thus necessary to categorise the diverse expressions and intensities of cracking into damage categories [16] and be able to quickly and objectively quantify and compare the intensity of damage between different cases or for different actions. For example, if only the crack width is used as a measure of damage, then the increase of the crack width can be related to the increase in damage; but, what happens if a second crack develops?

Consequently, a strict, mathematical definition of crack-based damage is herein proposed to objectively quantify damage in masonry structures. The goal of this definition is to assess the initiation, and most importantly, the progression of damage over time or during laboratory or computational experiments. Moreover, this is complemented with a high-resolution implementation of Digital Image Correlation [11] tailored to the evaluation of masonry cracks in laboratory tests. The usage of this definition allows for a more precise evaluation of light damage potentially caused by seismic events in the north of the Netherlands.

2. The Ψ Damage Parameter

2.1. Definition

Cracks in a masonry structure appear when the masonry tensile strength is exceeded [6]. Since masonry has a very low tensile strength, cracks are reasonably likely to appear in any structure; however, for a crack to be detectable it also needs to widen. Hence, deformations also need to take place. In Figure 1, an example of a wall with an opening subjected to a lateral load in its plane is presented. As the lateral force increases, so does the displacement measured at the top of the wall. This elastic relationship starts to degrade as the displacement increases at a larger rate than the force. This is linked to the appearance of crack(s) somewhere in the wall. Damage States, as defined by [8, 16], are usually employed to categorise the damage in the wall but these are not directly related to the cracks. After the wall reaches its maximum force capacity, cracks will become wider and failure will ultimately occur. Yet, the aggravation of cracks within the states up to DS2 is difficult to assess from force-displacement graphs, while also problematic to quantify using qualitative definitions for DS1 and DS2.

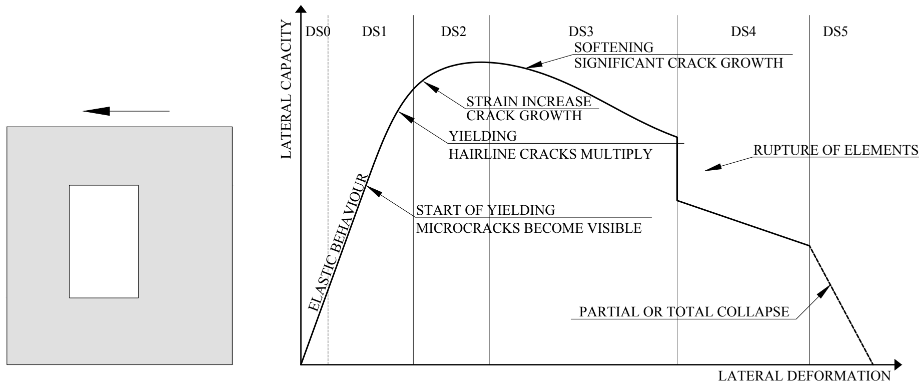

Figure 1. Typical initiation and propagation of cracks illustrated on a lateral force-displacement curve of a masonry wall.

Therefore, the summative crack pattern is better characterised with a parameter directly computed from the properties of the cracks. As mentioned before, the width of the cracks can be related to the intensity of the damage; however, the number of cracks is also influential. The assessment of laboratory specimens and inspection of real-world damage cases [15, 16] led to the realisation that cracks narrower than 0.1mm were difficult to see with the naked eye. In fact, from an anatomical perspective, the normal human eye can detect differences of down to 30μm in ideal light and contrast conditions (see for instance, [13]). Since cracks in masonry walls do not satisfy these ideal conditions even during rigorous inspections of plastered walls, a limit of 100μm was deemed reasonable, especially considering that the outer walls in Groningen masonry are mainly unplastered; and, since DS1 is related to aesthetic damage, damage that cannot be observed, is thus not relevant. This boundary is also employed as a cut-off value when measuring the length of cracks. Hence, a width of 0.1 mm was set as the lower boundary, below which no damage could be assumed.

The parameter that determines the damage intensity is herein based on the number, width, and length of the cracks following equation 1. The damage parameter Psi (Ψ) is based on a scale that defines the ease of repair of the cracks (adapted from Boscardin et al. [1], Burland et al. [2], and, at its latest, Giardina et al. [7]); see Table 1. Here, the total of visible cracks is expressed in one number such that the narrowest visible cracks with a width of 0.1 mm result in a value of around one (Ψ=1), slightly larger cracks of close to 1 mm width correspond to two (Ψ=2) and cracks of approximately 4 mm in width give a value of three (Ψ=3). This range of visible cracks from Ψ=1 to Ψ=3 is herein described as light damage (DS1). In this manner, Psi (Ψ) can be computed from both DIC and FEM data analogously: in the former by differentiating the displacement fields to obtain the crack width, and in the latter by employing the crack width data directly produced by finite element models with cracking material models.

$$\Psi = 2 \cdot n_c^{0.15} \cdot \hat{c}_w^{0.3} \text{ with} \hat{c}_w = \frac{\sum_{i=1}^{n_c} c_{w,i}^2 \cdot c_{L,i}}{\sum_{i=1}^{n_c} c_{w,i} \cdot c_{L,i}} \quad \text{(eq. 1)}$$

Where:
n_c is the number of cracks in the wall/specimen
$\hat{c}_w$ is the width-weighted and length-averaged crack width (in mm) calculated with:
c_w is the maximum crack width along each crack in mm
c_L is the crack length in mm
For n_c=1, $\hat{c}_w = c_w$. In this expression, the crack width of each crack is measured at their widest point.

Table 1. Definition of the Ψ Parameter

Category of damage	Damage		Description of typical damage and ease of repair	Approx. crack width (mm)
Aesthetic damage (DS1)	**Negligible**	**DL1**	Hairline cracks.	up to 0.1mm
	Very slight	**DL2**	Fine cracks which can easily be treated during normal decoration. Perhaps isolated slight fracturing in building. Cracks in external brickwork visible on close inspection.	up to 1mm
	Slight	**DL3**	Cracks easily filled. Redecoration probably required. Several slight fractures showing inside of building. Cracks are visible externally and some repainting may be required externally to ensure water tightness.	up to 5mm

The parameter equation is graphically shown in Figure 2 for some values of 'n_c'. The exponents (0.15 and 0.30) and coefficient (2) in the expression (equation 1) are tuned such that the relationship to the damage levels shown in Table 1 is maintained. Since these are qualitative descriptions, the defining expression of Ψ can be made to fit nicely. It is evident that a specimen or wall with multiple cracks is more damaged than one with a single crack. Moreover, Figure 3 gives a few examples of the usage of this parameter; one of the illustrated cases exceeds light damage and would probably better evaluated using a different kind of damage metric.

Nonetheless, the Ψ parameter allows for the comparison of the intensity of damage regardless of the specimen size. This is in-line with the parent damage scale (DS1-DS5), where the damage states are independent of the size of the structure and only the importance of the damage to each specific structure is considered. This is particularly advantageous when observing the progression of damage, and comparing it between samples of different dimensions. This parameter has been employed so far in several linked studies [15, 20, 21, 22]. Furthermore, since Ψ is related to the ease of repair of the damage, when the parameter is multiplied by the area of the affected wall, then a direct relationship to the cost of the repair can be obtained. This is treated later on.

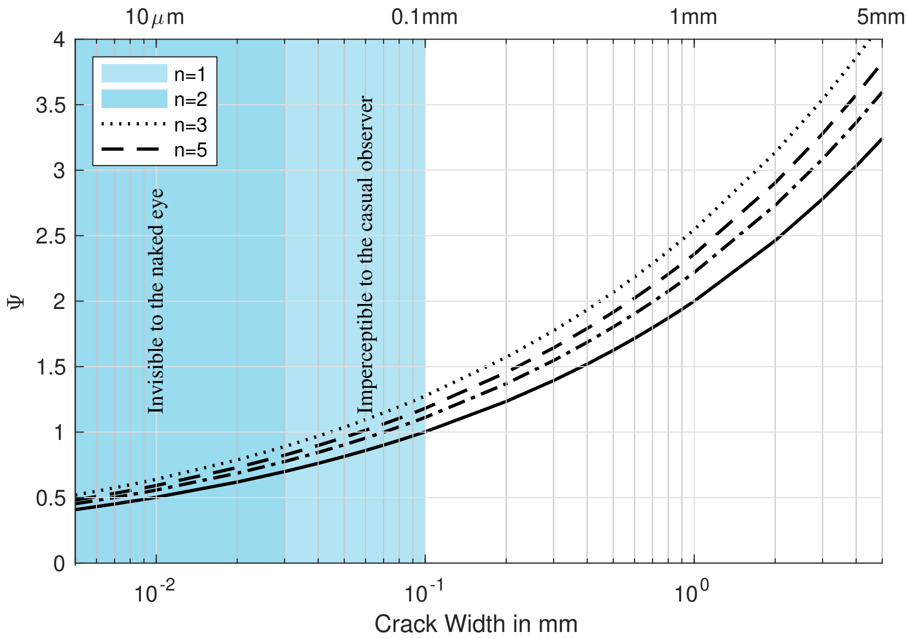

Figure 2. Illustration of the Ψ damage parameter against crack width and for different numbers of cracks.

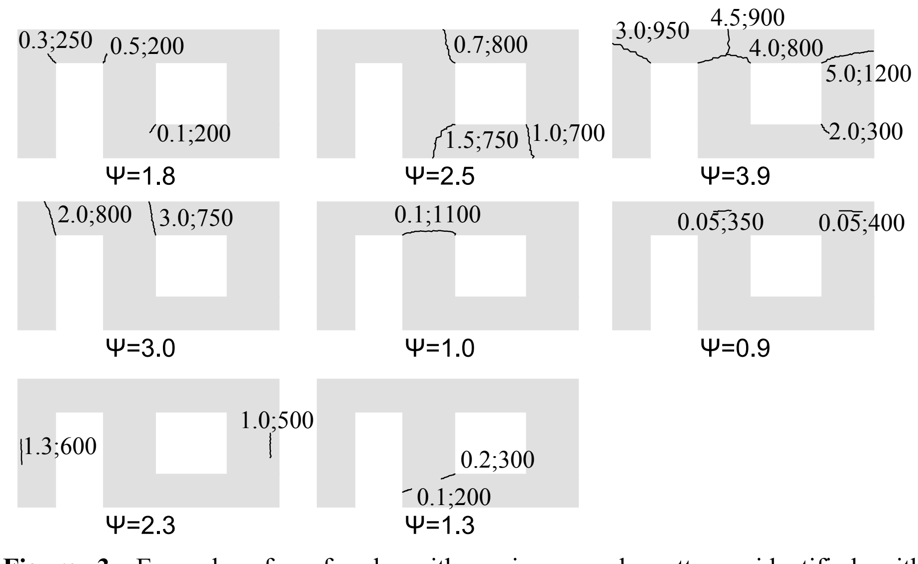

Figure 3. Example of a façade with various crack patterns identified with 'width;length' in millimetres, and labeled with the computed value of Ψ.

2.2. Limitations

Since damage is directly evaluated independently of the crack configuration, the progress (or intensification) of damage can be observed throughout experiments. Nevertheless, the use of one parameter to characterise the entire damage picture of a specimen is accompanied by certain limitations.

First, there is the loss of cause as the mechanism observed in a crack pattern cannot be captured in the value of one parameter. Second, in some cases, there is a loss of veridicality: Some changes such as the increase in length of one narrow crack while observing no changes in any other cracks, will produce an unexpected change in the value of Ψ. This is an unrealistic situation for which the parameter has not been calibrated. Such changes, however, have a small influence in the value of Psi and will be limited to a centesimal change. This leads to a loss of precision, but helps to realise that attempting to capture aesthetic damage with a high precision is not sensible.

In this light, the parameter needs always to be evaluated within realistic scenarios. For example, masonry walls are subjected to a limited number of cracks: attempting to evaluate Ψ with a high number of cracks is hence unrealistic. Moreover, since the parameter is related to the ease of repair, which in turn is related to the width of the cracks and not to their length, as was shown in Table 1, an extension in crack length will not necessarily lead to an increase in Ψ; in masonry, a significant increase in length is accompanied by a realistic increase in width, which is then reflected by a higher Ψ value.

Furthermore, when considering the definition of damage based on an observable measure of damage, “transitory damage” must be discussed. Transitory damage will differ from the actual damage level of a structure. As its name suggests, transitory damage reflects the state of a structure at a certain point in time and may not be the same as the damage state at the moment of observation. For example, during an earthquake, a structure may deform such that cracks of 1mm appear on the walls at the moment of maximum deformation; but, by the end of the earthquake, the cracks may have partially closed. If a picture had been taken at the moment of maximum deformation, the damage level would likely appear higher than the residual damage state. In this study, damage is analogous to transitory damage. This is a conservative approach yet especially suited for light damage due to the following reasons:

Firstly, unlike larger cracks exceeding DS1 which may close significantly compared to their maximum transitory state, narrower cracks corresponding to DS1 are not able to close once open because of the roughness of the newly developed crack interface. Moreover, cracks through bricks or in finished walls are irreversible: once a crack appears it will remain visible. Thus, when observing light damage, transitory and residual damage are more alike.

Secondly, since unreinforced masonry is designed without taking into account its tensile strength, it is usually not subjected to forces that would keep the cracks open once they have formed. However, when additional tensile stresses in more directions are present, such as those generated by hygro-thermal expansion or settlement actions, small cracks are more likely to remain open after they have formed. Additionally, unlike laboratory experiments where a restitutory force may exert the work required to close the cracks, in real cases, such a force may not be present; in fact, in real cases, forces might be present that keep the cracks open [15].

Thirdly, in contrast to field cases, observing transitory damage in laboratory experiments is possible and easier than the sometimes hardly-noticeable residual damage of lightly damaged cases subjected to only one action. Here, transitory damage will be higher than residual damage, and it is not possible to determine what the actual residual damage would have been, had the laboratory case been a real case in the field with complex interactions with other structural or non-structural elements and finishings. Furthermore, the maximum (transitory) and residual damage can also be obtained easily from computational models, which provides an additional point of comparison.

Fourthly, when analysing the effect of a combination of actions or of repeated actions, the true damaged state of the structure is that revealed by the maximum transitory state. The transitory state will be a more accurate representation of the loss of strength experienced by the structure and hence its response to subsequent excitations. The analysis of the behaviour of the structure to subsequent damage causes or events should be performed with the maximum damage and not the (perhaps inapparent) residual damage. Thus, when multiple damaging causes are considered, the residual damage would not be adequately suited.

Fifthly, when considering the structural design of a structure and whether it adheres to regulations, drift limits are specified towards the maximum displacement of the structure and not the residual displacement. It is thus common practice to look at the maximum transitory state of a structure when assessing its final damage state.

Therefore, transitory damage was used consistently in this study when referring to damage, and while it is expected that for light damage, the transitory damage will be close to the final damage, it must be noted that the final damage is bound to be slightly lower than the transitory damage measure employed.

2.3. Perception of Damage

Two identical houses subjected to similar actions will be similarly damaged; however, if one house has walls covered in a plaster that is old and stiff while the other has walls covered in flexible wallpaper, the former will display any crack prominently, while the latter will hide cracks. The first house will be perceived to be more damaged than the second one. This is the perceived damage state which may differ from the actual damage state.

This work focuses on real damage and observes the physical processes that lead to it, but it is still important to acknowledge that damage can be subjective and that certain combinations of architectural building parameters will lead to more reported damage. Understanding how damage is likely to be perceived also gives insight into overall damage conditions in the region.

The following is an empirical proposal of how and which parameters relating to the aesthetic and architectural disposition of the structure, as well as the situation in which damage was observed, may affect the way in which damage is perceived.

$$\psi = \Psi^{\frac{k}{3}} \quad \text{(eq. 2)}$$

Where:
ψ is the perceived damage intensity (lowercase Ψ)
Ψ is the damage parameter (uppercase Ψ)
k is the average of the empirically-determined influence parameters for each category as shown in Table 2.

It is possible to include as many categories as deemed relevant into the evaluation of the perception of damage. Additionally, the relation can be inverted to try to estimate the actual damage of a structure from a study case report. In the former case, an estimation of how damage will be perceived can be inferred from a numerical model, while in the latter, a more accurate estimation of damage can be registered from an uncertain field report.

2.4. Agglomeration of Psi

The Ψ parameter has been mainly developed to assess the progression of damage on a certain specimen or between identical specimens. However, sometimes different walls or structures would like to be compared to each other to determine which presents lower or higher damage. In this case, it is convenient to express a relative version of Ψ based on the surface area of the masonry:

$$\Psi_i' = \Psi_i \cdot \frac{A_i}{\bar{A}} \qquad \text{(eq. 3)}$$

Where A_i is the surface are of the wall i, $\bar{A}$ is the mean area of the walls considered and Ψ' is the relative Ψ. Furthermore, if a structure where each wall is monitored separately wants to be characterised with a single value of Ψ, the damage in the N walls can be accounted as:

$$\bar{\Psi} = \frac{\sum_{i=1}^{N} \Psi_i \cdot A_i}{A_T} \qquad \text{(eq. 4)}$$

Where $\bar{\Psi}$ is the mean Ψ value and A_T is the sum of the surface areas.

3. Digital Image Correlation for Cracks

Photogrammetry techniques can be used to automatically detect cracks [12, 19, 28]. Digital Image Correlation (DIC) is widely used in laboratories to measure displacement and strains on small samples or large surfaces where the use of multiple sensors is inconvenient [11, 14]. However, strains are not easily linked to cracks. Usually, measured strains are smoothed out over a certain surface to correct for noise and the relatively low resolution of DIC. The smooth strains are thus not representative of the discrete cracks appearing on masonry specimens.

As part of the experimental validation of the usage of the Ψ parameter, cracks had to be automatically detected to assess the progression of damage over hundreds of loading cycles [22]. For this purpose, a 51 Mpx DSLR camera and a 35mm lens stopped down to f/9.0 were used to acquire high resolution images. Shots were illuminated with a flash at a speed of 1/63000s to produce even lighting conditions and eliminate image blur. The setup, in combination with an optimised speckle pattern

[3] and the DIC-algorithm developed for these kind of tests, allowed for the observation of the initiation and, most importantly, the progression (in width and in length) of cracks invisible to the naked eye over the entire surface of a full-scale wall. Figure 4 presents an example of a 2.7m-tall masonry wall covered in a speckle pattern where dots are randomly positioned and randomly vary in diameter between 4 and 8 pixels. To produce such a pattern, a stencil was laser-cut from a flexible acrylic plate and was applied on the masonry by spraying black paint with a compressed-air nozzle, similar to the approach of Ghorbani et al. [25]. The random pattern was generated with a script that allowed changing the sizes and distances of the dots. Multiple patterns were tested on small specimens to determine the best set of parameters. The pattern allows a (standard) DIC-algorithm to detect the relative displacements between an initial image and a later image. In Figure 4, the displacement field reveals the presence of cracks. The DIC pattern on the wall in combination with the camera allowed for the monitoring of the full displacement field of the wall in a grid with a spacing of 2.6x2.6 mm and a precision of 20 µm, comprising over 1.2 million measurement (or grid) points. Images were taken at precise time-points throughout the test. The accuracy of the setup allows to detect displacements as small as a fifth of the threshold set for visible cracks; this has herein been considered as high-resolution.

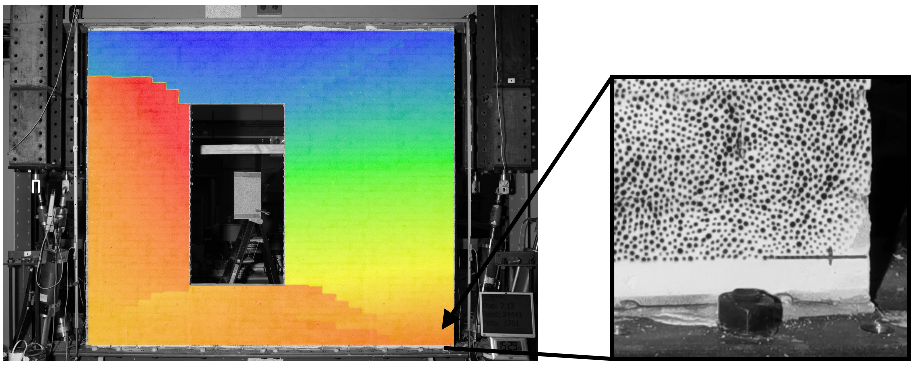

Figure 4. Laboratory wall specimen (3.1m x 2.7m) overlaid with the horizontal displacement field obtained with DIC during testing of a lateral top displacement in-plane. Right, zoomed-in corner of the wall depicting the speckle pattern used for DIC.

The raw or unmodified displacement field acquired by a DIC-algorithm using small subsets (of approximately 10 pixels) to avoid smoothing the displacement values, can be scanned for discontinuities above a certain threshold; large groups of discontinuities are likely to correspond to cracks. The relative displacement between one side of the discontinuity and the other corresponds to the width of the crack. Figure 5 presents the result of this operation where each crack is automatically characterised in width and length. Note that the wall specimens of Figure 4 and Figure 5 are not the same. While many authors utilise strains to map cracks [25, 26, 27, 28], strains would need to be integrated over a crackbandwidth to be able to output the crack width and length, and can thus only be used in an illustrative manner. The detection and characterisation of discontinuities, on the other hand, is much better tailored to obtain the crack kinematics. Gehri et al. [24] specify this approach in detail. The resulting data can provide an in-depth look at crack progression; Figure 6 presents the crack width at the centreline of the crack over multiple experimental cycles. It can be observed that the crack grows in width and in length throughout the experiment. The centreline is captured automatically by following the trend of the maximum width over the crack. It can also be seen that the DIC output is not free from noise; however, with thousands of measurement points over the crack, reasonable values can be computed.

For each frame in the experiment, with crack widths and lengths determined, the Ψ value is computed as in Figure 7. This illustrates how Ψ increases throughout the experiment, even during cycles of equal amplitude.

While the algorithm employed here was custom-written to detect cracks with the highest accuracy possible, commercial DIC tools have started to implement crack-oriented solutions [23] and it remains convenient to tailor solutions to specific experiments [24]. These analysis tools will allow for an easier characterisation of light damage in masonry.

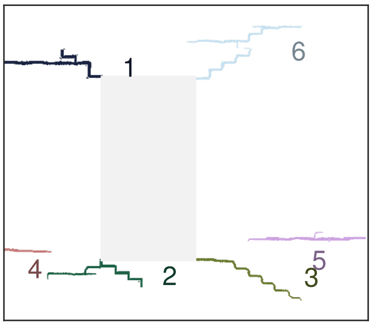

Crack	Width (µm)	Length (mm)
1	750	980
2	285	866
3	361	1278
4	375	445
5	676	1052
6	482	1330

Figure 5. Detected cracks in DIC data of a laboratory masonry wall.

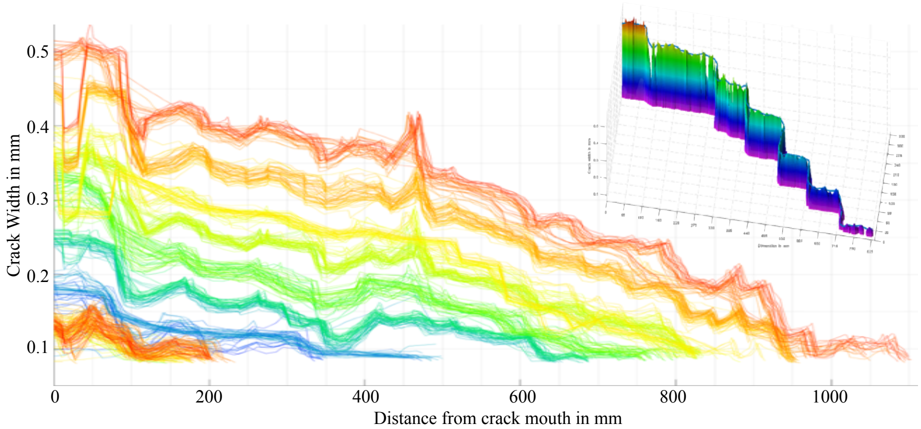

Figure 6. Crack width against crack length as measured by the centreline of the crack, for numerous test cycles.

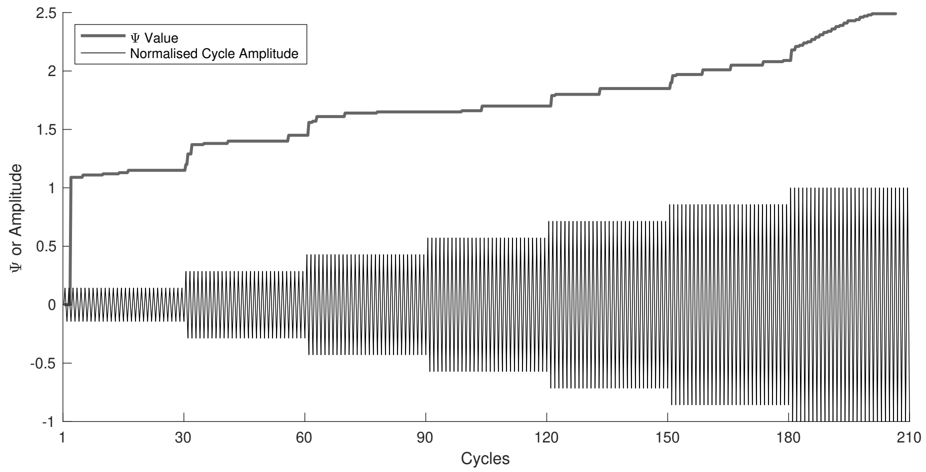

Figure 7. Development of the Ψ value throughout testing of a wall indicating also the progression of the amplitude of the applied lateral top displacement.

4. Conclusions

Digital Image Correlation can be used successfully for the crack characterisation of laboratory masonry walls. The resolution achieved is sufficient for the accurate assessment of crack propagation even during repeating cycles of equal amplitude. The aggravation of damage can then be measured using a purposely-developed parameter that considers the number of cracks on the wall specimen, their width and their length. The parameter can be used to compare the damage progression even when cracks increase in number.

Acknowledgements: This research was funded by Nederlandse Aardolie Maatschappij (NAM) under contract number UI67339 'Damage sensitivity of Groningen masonry building structures – Experimental and computational studies', contract holders: Jan van Elk and Jeroen Uilenreef. This cooperation is gratefully acknowledged.

5. References

1. M.D. Boscardin, E.J. Cording (1989). Building response to excavation-induced settlement. Journal of Geotechnical Engineering, 115(1):1–21, 1989.
2. J.B. Burland, C.P. Wroth (1974). Settlement of buildings and associated damage. Proceedings of Conference on Settlement of Structures, pages 611–654, Cambridge, 1974. Pentech Press.
3. G. Crammond, S.W. Boyd, J.M. Dulieu-Barton (2013). Speckle pattern quality assessment for digital image correlation. Optics and Lasers in Engineering 51 (2013) 1368–1378

4. M. Didier, G. Abbiati, M. Broccardo, K. Beyer, L. Danciu, M. Petrović, N. Mojsilović, B. Stojadinović (2017). Quantification of Non-Structural Damage in Unreinforced Masonry Walls Induced by Geothermal Reservoir Exploration using Quasi-Static Cyclic Tests. Proceedings of the 13th Canadian Masonry Symposium, Halifax, Canada, June 2017
5. M. Didier, G. Abbiati, F. Hefti, M. Broccardo, B. Stojadinovic (2018). Damage Quantification In Plastered Unreinforced Masonry Walls Using Digital Image Correlation. 10th Australasian Masonry Conference, 14-18 February, 2018
6. N. Gattesco, L. Macorini, A. Dudine (2016). Experimental Response of Brick-Masonry Spandrels under In-Plane Cyclic Loading. ASCE Journal of Structural Engineering Vol. 142, Issue 2 (February 2016).
7. G. Giardina, A.V. van de Graaf, M.A.N. Hendriks, J.G. Rots, A. Marini (2013). Numerical analysis of a masonry façade subject to tunnelling-induced settlements. Engineering Structures 54 (2013) 234–247
8. G. Grünthal (1998). European Macroseismic Scale 1998 (EMS-98). European Seismological Commission, sub commission on Engineering Seismology, Working Group Macroseismic Scales. Conseil de l'Europe, Cahiers du Centre Européen de Géodynamique et de Séismologie, Vol. 15, Luxembourg.
9. S. Jafari, R. Esposito, J.G. Rots, F. Messali (2017). Characterizing the Material Properties of Dutch Unreinforced Masonry. Procedia engineering, 193, 250-257
10. P.A. Korswagen, S.N. Jonkman, K. Terwel (2019). Probabilistic assessment of structural damage from coupled multi-hazards. Structural Safety Volume 76, 2019, pgs 135-148, ISSN 0167-4730, https://doi.org/10.1016/j.strusafe.2018.08.001
11. F. Laurin, J.S. Charrier, D. Lévêque, J.F. Maire, A. Mavel, P. Nuñez (2012). Determination of the properties of composite materials thanks to digital image correlation measurements . Procedia IUTAM 4 (2012) 106 – 115
12. N. Mojsilović, A.H. Salmanpour (2016). Masonry walls subjected to in-plane cyclic loading: Application of Digital Image Correlation for deformation field measurement . Institute of Structural Engineering, Department of Civil, Environmental and Geomatic Engineering, ETH Zurich, 8093, Switzerland
13. G. Österberg (1935). Topography of the layer of rods and cones in the human retina. Acta Ophthalmol [Suppl] 13:6,1–102
14. T. Ramos, A. Furtado, S. Eslami, S. Alves, H. Rodrigues, A. Arêde, P. Tavares, P. Moreira (2015). 2D and 3D Digital Image Correlation in Civil Engineering – Measurements in a Masonry Wall. Procedia Engineering 114 (2015) 215 – 222
15. P. Van Staalduinen, K. Terwel, J.G. Rots (2018). Onderzoek naar de oorzaken van bouwkundige schade in Groningen Methodologie en case studies ter duiding van de oorzaken. Delft University of Technology. Report number CM-2018-01, 11 July 2018 - Downloadable from www.NationaalCoordinatorGroningen.nl
16. I. de Vent, J.G. Rots, R.P.J. van Hees (2011). Structural Damage in Masonry - Developing diagnostic decision support. TU Delft
17. J. Blaber, B. Adair, A. Antoniou (2015). Ncorr- Open-Source 2D Digital Image Correlation Matlab Software. Experimental Mechanics DOI 10.1007/s11340-015-0009-1
18. V. Bosiljkov, A.W. Page, V. Bokan-Bosiljkov, R. Zarnić (2008). Evaluation of the seismic performance of brick masonry walls. Struct. Control Health Monit. 2010; 17:100–118 Published online 22 December 2008 in Wiley InterScience (www.interscience.wiley.com). DOI: 10.1002/stc.299

19. M. Dhanasekar, P. Prasad, J. Dorji, T. Zahra (2019). Serviceability Assessment of Masonry Arch Bridges Using Digital Image Correlation. J. Bridge Eng., 2019, 24(2): 04018120
20. P.A. Korswagen, M. Longo, E. Meulman, J.G. Rots (2019). Crack initiation and propagation in unreinforced masonry specimens subjected to repeated in‑plane loading during light damage. Bulletin of Earthquake Engineering https://doi.org/10.1007/s10518-018-00553-5
21. P.A. Korswagen, M. Longo, J.G. Rots (2020). High-resolution monitoring of the initial development of cracks in experimental masonry shear walls and their reproduction in finite element models. Engineering Structures 211 (2020) 110365
22. P.A. Korswagen, M. Longo, J.G. Rots (2020). Calcium silicate against clay brick masonry: an experimental comparison of the in‑plane behaviour during light damage. Bulletin of Earthquake Engineering 18, 2759–2781 https://doi.org/10.1007/s10518-020-00803-5
23. GOM Correlate - visited June 2020. www.gom.com/3d-software/gom-correlate/gom-correlate-features.html#video51438
24. N. Gehri, J. Mata-Falcón, W. Kaufmann (2020). Automated crack detection and measurement based on digital image correlation. Construction and Building Materials 256 (2020) 119383
25. R. Ghorbani, F. Matta, M.A. Sutton (2015). Full-Field Deformation Measurement and Crack Mapping on Confined Masonry Walls Using Digital Image Correlation. Experimental Mechanics (2015) 55:227–243
26. S.L. Kumar, H.B. Aravind, N. Hossiney (2019). Digital image correlation (DIC) for measuring strain in brick masonry specimen using Ncorr open source 2D MATLAB program. Results in Engineering 4 (2019) 100061
27. M.F. Smrkić, J. Košćak, D. Damjanović (2018). Application of 2D digital image correlation for displacement and crack width measurement on RC elements. Građevinar 70 (2018) 9, 771-781
28. S. Tung, M. Shih, W. Sung (2008). Development of digital image correlation method to analyse crack variations of masonry wall. Sadhana Vol. 33, Part 6, December 2008, pp. 767–779.

6. Appendix

Table 2. Influence values for various non-structural aspects influential in damage perception. Empiric exemplary values.
1 - Reduces the perception of damage significantly; 2 - Reduces the perception of damage; 3 - Does not influence; 4 - Increases the perception of damage; 5 - Increases the perception of damage significantly.

Category	Subcategories	Influence Value (k)	Description
Age	very old	2	Older than 1970
	older	3	Between 1970 and 2000
	new	4	Newer than 2000
Material	baked clay	3	
	calcium silicate	4	
Wall type	slim	4	Less than 120mm
	thick	3	Greater than 120mm
	double	2	More than one layer of bricks
Cavity	without cavity	3	One single leaf
	cavity and aesthetic	4	Two leaves, where only one is structural
	cavity and structural	3	Two leaves, both structural
Brick Type	regular bricks	3	units with a height smaller than 150mm
	large blocks	4	units with a height larger than 150mm
	hollow units	3	units that are not solid
Mortar	slim	4	the joints are around 3mm according to EC
	free verticals	2	vertical joints between the bricks are not filled
	normal	3	all joint are filled and greater than 3mm
Finish	exposed	2	the bricks and joints can be seen
	plaster + paint	3	the wall is covered with plaster and painted
	mortar + paint	4	the wall is covered with mortar and painted
	elastomeric paint	2	wall is (covered and) painted with flexible paint
	Wall paper	1	the wall is plastered and covered with paper